Quantum Dots

DOI: 10.1002/anie.201406330

Size-Dependent Thermochromism through Enhanced Electron–Phonon Coupling in 1 nm Quantum Dots**

*Haruna Tamaki, Hiroto Watanabe, Sachiko Kamiyama, Yuya Oaki, and Hiroaki Imai**

Abstract: *1 nm CuO quantum dots (QDs) were produced in size-controlled super-micropores of a silica matrix. The reversible color change of the QDs from pale blue to deep green was clearly observed in a wide temperature range from 298 to 673 K. This particular thermochromism is ascribed to an enhanced bandgap shift depending on temperature with a strong electron–phonon coupling in the confined space of the 1 nm QDs.*

Thermochromism, reversible and visible color change with temperature variation, has been attracting interest for a long time.[1–3] The reversible and visible color change is utilized for various applications, such as solar protection, and thermal indicators.[1,2] The mechanism of the thermochromism depends on the type of material. For example, the color change of several organic substances is attributed to an equilibrium between two molecular species, two stereoisomers, or two crystal structures.[1] The distinct thermochromism of inorganic transition-metal salts is generally ascribed to phase transitions.[2] On the basis of the mechanisms, the color change of a wide variety of thermochromic materials occurs at a certain transition temperatures below approximately 500 K. Although a gradual color change of ZnO from white to yellow is observed in a wide temperature range of 10–800 K,[3] the thermochromism that originates from the bandgap shift is not highly visible owing to the small temperature coefficient α (0.6 meV/K). Herein, we report thermally stable, visible, and gradual thermochromism in a wide temperature range, from 298 to 673 K, on 1 nm CuO quantum dots (QDs) produced in super-microporous silica (SMPSs).

[*] H. Tamaki, Dr. H. Watanabe, S. Kamiyama, Dr. Y. Oaki, Prof. Dr. H. Imai
Department of Applied Chemistry
Faculty of Science and Technology, Keio University
3-14-1 Hiyoshi, Kohoku-ku, Yokohama 223-8522 (Japan)
E-mail: hiroaki@applc.keio.ac.jp
Dr. H. Watanabe
Material Technology Group
Tokyo Metropolitan Industrial Technology Research Institute
2-4-10 Aomi, Koto-ku, Tokyo 135-0064 (Japan)

[**] This work was supported by Grant-in-Aid for Scientific Research (B) (23350102) Grant-in-Aid for Scientific Research (B) (23350102), the Ministry of Education, Culture, Sports, Science and Technology, and Tokyo Metropolitan Collaboration of Regional Entities for the Advancement of Technological Excellence (Japan) Science and Technology Agency (JST). We are grateful to Mr. T. Mitani for his help in FE-TEM measurement and Dr. S. Somekawa for his help in XPS measurement.

Supporting information for this article is available on the WWW under http://dx.doi.org/10.1002/anie.201406330.

QDs have attracted considerable attention because of their unique size-dependent properties, such as photoluminescence,[4] intrinsic magnetism,[5] and electrochemical characteristics,[6] which deviate significantly from those of their bulk states due to the quantum-size effect.[7] These novel properties show great potential as sensors,[8] photocatalysts,[9] optoelectronic devices,[10] and for various biological and medical applications.[4] Although temperature dependence of the bandgap and photoluminescence was reported for QDs,[11,12] thermochromism enhanced by the quantum-size effect has not been reported for metal oxides.

Single nanosized QDs have been synthesized by various methods, such as laser ablation,[7,13] organometallic chemical synthesis,[14] and with designed dendrimers.[15] However, size-controlled synthesis of sub-nanosized QDs below approximately 1 nm has been difficult using conventional methods. Strong quantum-size effects are usually observed on single nanosized QDs, such as CdS, CdSe, and CdTe.[14] On the other hand, the QD size must be lowered to approximately 1 nm to observe significant effects for most transition-metal oxides because of their small exciton Bohr radius.[9,15] Therefore, size-controlled synthesis in the range around 1 nm is required to utilize the enhanced properties of the metal oxides.

Porous materials, such as zeolites[16] and mesoporous silicas (MPSs),[17,18] are used as a template for the synthesis of QDs because the pore size can control the dot size. However, coexistence of the pore windows and large cages restricts the uniformity of QDs prepared in zeolites. In contrast, using MPSs has many advantages, such as controllability of the narrow particle-size distribution. However, the synthesis of sub-nanosized QDs below 1 nm has rarely been achieved because of the difficulty in controlling the pore size in the super-micropore region (0.7–2.0 nm).[19] Recently, our group produced SMPSs by the solvent-free synthetic method.[9] In our previous research, size-controlled WO_3 QDs (0.7–1.8 nm) were synthesized using SMPSs as templates. The bandgap varied from 2.6 (bulk) to 3.7 eV (0.7 nm QD) owing to the quantum-size effect. Moreover, enhancement of the photocatalytic ability with the bandgap expansion was demonstrated.

CuO is an indirect semiconductor with a bandgap of approximately 1.3 eV.[20] The oxide semiconductor has been studied for various application fields, such as photocatalysts,[21] sensors,[22] and lithium-ion batteries.[23] The nanoparticles of CuO were synthesized through various routes, such as a hydrothermal method,[22] electrochemical fabrication,[24] and flame spray pyrolysis,[23] to enhance their performance. Although the templating method using MPSs has been reported, the lower limit of the particle size prepared in the mesopores was approximately 3.0 nm.[25]

In the present study, CuO QDs were synthesized in porous silicas with pores from 0.64 to 1.69 nm in diameter. The bandgap of the CuO QDs steeply increased as their size decreased below 2 nm. Moreover, the color of the QDs reversibly varied with changing temperature in the range from 298 to 673 K, whereas visible thermochromism cannot be observed in bulk CuO. This interesting phenomenon that originates from the bandgap shift's dependence on temperature is ascribed to the strong electron–phonon coupling that is enhanced in the confined space of the 1 nm QDs. Three kinds of porous silicas, listed in Table 1, were used as templates for the production of CuO QDs (C4, C8, and C12). More information about porous silicas is provided in the Supporting Information (Figure S1 and Table S1). As shown in the typical STEM images (Figure 1), many black spots can be observed in the silica matrix. The average sizes of the spots estimated from the images nearly agree with the pore size of the templates (Table 1). Signals assigned to silicon and copper were detected by energy-dispersive X-ray spectroscopy (EDX). The value of the $2p_{3/2}$ binding energy and the appearance of two satellite peaks in an X-ray photoelectron (XPS) spectrum for C12 (Figure S2) indicate the presence of CuO in the silica matrix.[26] According to these results, we successfully synthesized CuO QDs whose particle size nearly agrees with the pore size of the silica templates.

Table 1: The porous silicas used as templates of CuO QDs.

Sample	Directing agent	Pore size [nm]	Particle size [nm]
C4	C4TAC	0.64	–[b]
C8[a]	C8TAB	0.87	1.05 ± 0.5
C12	C12TAB	1.69	1.65 ± 0.8

[a] A mixture of TEOS and TEVS was used as a silica source for adjusting the pore size. [b] The particle size was not clearly defined owing to weak contrast of the image for sub-nanometer dots in C4.

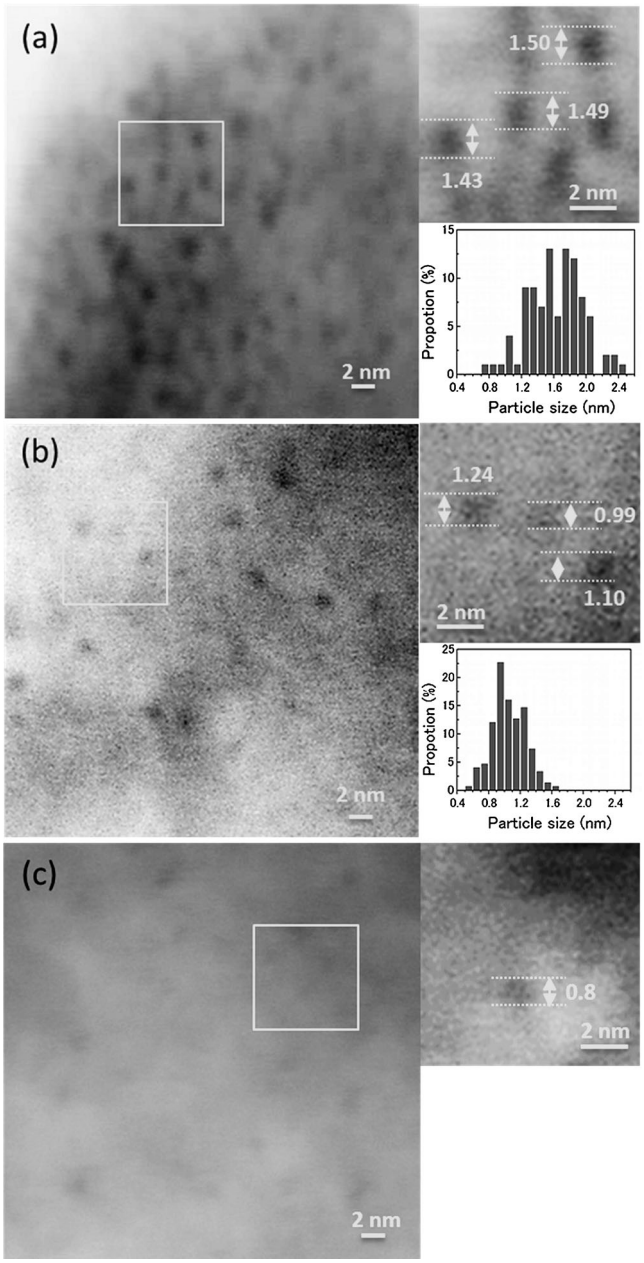

Figure 1. Representative STEM images and histograms of particle size estimated from the images. a) C12, b) C8, and c) C4. The average diameters of the dots in C12 and C8 were estimated to be 1.65 and 1.05 nm, respectively. The size of dots in C4 seems to be below 1 nm, but was not clearly defined owing to the weak contrast of the image. These pictures were obtained from STEM images by contrast inversion for clear visualization.

Figure 2a shows distinct, gradual variation of the color and the UV/Vis spectra of the CuO QDs in the porous silica matrix with the change in the pore size of the templates. This variation is attributed to a remarkable blue shift of the absorption edge as a result of a bandgap expansion of the CuO QDs. A broad signal of around 750 nm is attributed to d–d transitions of Cu^{2+} surrounded by oxygen in CuO.

Figure 2b shows the bandgap energy of the CuO QDs obtained from the Tauc plot (Figure S4 in the Supporting Information).[27] The theoretical size-dependence of the bandgap of CuO was estimated using the Brus equation [Eq. (1)],[28]

$$E_g(r) = E_g(\infty) + \frac{h^2}{8r^2}\left(\frac{1}{m_e} + \frac{1}{m_h}\right) \quad (1)$$

where r is the particle radius, $E_g(\infty)$ is the bandgap energy of bulk, h is the Planck constant, m_e is the effective mass of the electron, and m_h is the effective mass of the hole. For CuO, 1.25 eV as $E_g(\infty)$, 1.96×10^{-30} kg as m_e, and 7.20×10^{-30} kg as m_h[20,29] were used for the calculation. Because the experimental data agreed with the theoretical values, the significant bandgap expansion of the CuO QDs is attributed to the strong quantum-size effect.

The color of CuO QDs depends on their size. Moreover, the distinct and reversible color change of the QDs is observed with temperature variation, as shown in Figure 3a. This thermochromism of CuO is ascribed to the shift of the absorption edge in the visible region. The temperature-dependent shift of the bandgap is essential for this color change. The UV/Vis spectra of all of the samples depending

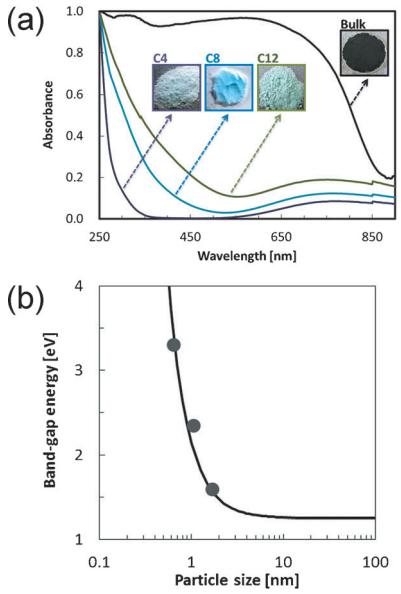

Figure 2. UV/Vis spectra, color, and bandgap energy of CuO. a) Normalized UV/Vis spectra and optical photographs of bulk CuO (black), and CuO QDs in the porous silica matrix (C12 (green), C8 (blue), C4 (purple)). b) The correlation between the bandgap of CuO QDs and their size. The black line represents the Brus equation [Eq. (1)], and circles represent experimental data. The pore size of the silica template is indicated instead of the particle size for C4.

on temperature are shown in Figure S5. As shown in Figure 3b and Figure S6, the bandgap energy of the CuO QDs depends on the temperature. The experimental data from 298 to 673 K were fitted by the Varshni equation (see Supporting Information)[30] and the O'Donnell and Chen equation [Eq. (2)].[11,12] From the Varshni equation, we determined

$$E_g(T) = E_g(0) - \frac{2S\langle\hbar\omega\rangle}{\exp(\langle\hbar\omega\rangle/k_B T) - 1} \quad (2)$$

the temperature coefficient α (Figure S7). The α values increased from 0.8 meV K^{-1} (bulk) to 2.3 meV/K (in C4) by decreasing the particle size of CuO QDs. These values are remarkably higher than the previously reported values of ZnO (0.6 meV K^{-1}) and QDs of InP (0.3–0.7 meV K^{-1}).[3,12] The bandgap shift is not attributed to the effect of lattice dilation itself or the quantum-confined energy shifts arising from the thermal dilation because of a small thermal expansion coefficient of CuO (ca. 6×10^{-6} K^{-1}).[31] Therefore, the experimental data were fitted by the O'Donnell and Chen equation based on an analysis of the specific mechanism causing bandgap narrowing, involving the electron-phonon coupling,[11,12]

where T is the temperature, $E_g(0)$ is the bandgap at 0 K, S is the Huang–Rhys factor, which reflects the electron–phonon coupling strength, $\langle\hbar\omega\rangle$ is the average phonon energy, and k_B is the Boltzmann constant. As shown in Figure 3c, the S values increase as the particle size is decreased.[12] The high values for the 1 nm CuO QDs suggest that the distinct thermochromism is ascribed to the electron–phonon coupling that is extremely enhanced in the confined space.

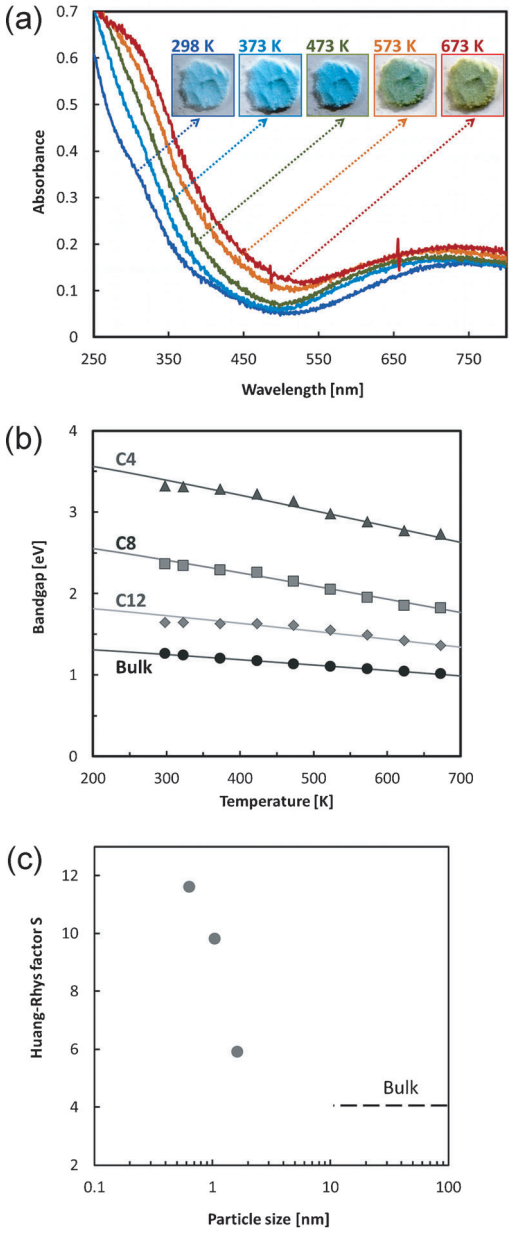

Figure 3. Dependence of UV/Vis spectra, color, and bandgap energy of CuO on temperature. a) UV/Vis spectra and optical photographs of C8 containing CuO QDs at different temperatures from 298 to 673 K. b) Temperature dependence of the bandgap of CuO QDs in the porous silica matrix (C4 (▲), C8 (■), C12 (◆)), and bulk CuO (●). Plots are experimental data and solid lines are obtained by the O'Donnell and Chen equation [Eq. (2)]. c) Dependence of the Huang–Rhys factor S on the particle size of CuO QDs. The pore size of the silica template is indicated instead of the particle size for C4.

The bandgap of bulk CuO changes slightly with temperature variation (Figure 3b), and the shift in the infrared region is invisible. On the other hand, the bandgap energy of CuO is drastically shifted to the UV region, because of the quantum size effect, by means of the formation of 1 nm QDs in the super-micropores of the silica matrix. The visible thermochromism from pale blue to deep green is clearly observed for the CuO QDs in the porous silica matrix because

of the significant expansion of the bandgap. Moreover, the distinct color change with temperature variation is enhanced with the strong electron–phonon coupling in the confined space.

In conclusion, we produced 1 nm CuO QDs in a super-microporous silica matrix. Thermally stable, visible, and gradual thermochromism was observed on the CuO QDs with significant bandgap expansion due to the quantum-size effects and the enhanced electron–phonon coupling.

Received: June 18, 2014
Published online: August 11, 2014

Keywords: microporous materials · quantum dots · template synthesis · transition metal oxide

[1] J. H. Day, *Chem. Rev.* **1963**, *63*, 65 – 80.
[2] D. R. Bloomquist, R. D. Willett, *Coord. Chem. Rev.* **1982**, *47*, 125 – 164.
[3] R. Hauschild, H. Priller, M. Decker, J. Bruckner, H. Kalt, C. Klingshirn, *Phys. Status Solidi C* **2006**, *3*, 976 – 979.
[4] I. L. Medintz, H. T. Uyeda, E. R. Goldman, H. Mattoussi, *Nat. Mater.* **2005**, *4*, 435 – 446.
[5] S. Tarucha, D. G. Austing, T. Honda, R. J. Van der Hage, L. P. Kouwenhoven, *Phys. Rev. Lett.* **1996**, *77*, 3613 – 3616.
[6] S. M. Cronenwett, T. H. Oosterkamp, L. P. Kouwenhoven, *Science* **1998**, *281*, 540 – 544.
[7] Y. Wang, N. J. Herron, *Phys. Chem.* **1991**, *95*, 525 – 532.
[8] H. Kuang, Y. Zhao, W. Ma, L. Xu, L. Wang, C. Xu, *TrAC Trends Anal. Chem.* **2011**, *30*, 1620 – 1636.
[9] H. Watanabe, K. Fujikata, Y. Oaki, H. Imai, *Chem. Commun.* **2013**, *49*, 8477 – 8479.
[10] S. A. McDonald, G. Konstantatos, S. Zhang, P. W. Cyr, E. J. D. Klem, L. Levina, E. H. Sargent, *Nat. Mater.* **2005**, *4*, 138 – 142.
[11] K. P. O'Donnell, X. Chen, *Appl. Phys. Lett.* **1991**, *58*, 2924 – 2926.
[12] A. Narayanaswamy, L. F. Feiner, A. Meijerink, P. J. Van der Zaag, *ACS Nano* **2009**, *3*, 2539 – 2546.
[13] K. Suzuki, M. Inoguchi, K. Kageyama, H. Sakabe, *J. Nanopart. Res.* **2009**, *11*, 1349 – 1360.
[14] C. B. Murray, D. J. Norris, M. G. Bawendi, *J. Am. Chem. Soc.* **1993**, *115*, 8706 – 8715.
[15] N. Satoh, T. Nakashima, K. Kamikura, K. Yamamoto, *Nat. Nanotechnol.* **2008**, *3*, 106 – 111.
[16] T. Frising, P. Leflaive, *Microporous Mesoporous Mater.* **2008**, *114*, 27 – 63.
[17] T. Yanagisawa, T. Shimizu, K. Kuroda, C. Kato, *Bull. Chem. Soc. Jpn.* **1990**, *63*, 988 – 992.
[18] J. S. Beck, J. C. Vatuli, W. J. Roth, M. E. Leonwicz, C. T. Kresge, K. D. Schmitt, C. T.-W. Chu, D. H. Olson, E. W. Sheppard, S. B. McCullen, J. B. Higgins, J. L. Shelenker, *J. Am. Chem. Soc.* **1992**, *114*, 10834 – 10843.
[19] J. M. Fedeyko, D. G. Vlachos, R. F. Lobo, *Microporous Mesoporous Mater.* **2006**, *90*, 102 – 111.
[20] D. X. Wu, Q. M. Zhang, M. Tao, *Phys. Rev. B* **2006**, *73*, 235206.
[21] S. C. Roy, O. K. Varghese, M. Paulose, C. A. Grimes, *ACS Nano* **2010**, *4*, 1259 – 1278.
[22] M. U. Anu Prathap, B. Kaur, R. Srivastava, *J. Colloid Interface Sci.* **2012**, *370*, 144 – 154.
[23] O. Waser, M. Hess, A. Guentner, P. Novak, S. E. Pratsinis, *J. Power Sources* **2013**, *241*, 415 – 422.
[24] H. Ming, P. Keming, L. Yang, L. Haitao, H. Xiaodie, M. Jun, M. Zheng, K. Zhenhui, *J. Cryst. Growth* **2011**, *327*, 251 – 257.
[25] P. Y. Wang, X. P. Zheng, X. Y. Wu, X. F. Wei, L. Zhou, *Microporous Mesoporous Mater.* **2012**, *149*, 181 – 185.
[26] N. S. Mcintyre, M. G. Cook, *Anal. Chem.* **1975**, *47*, 2208 – 2213.
[27] J. Tauc, *Mater. Res. Bull.* **1970**, *5*, 721 – 730.
[28] L. Brus, *J. Phys. Chem.* **1986**, *90*, 2555 – 2560.
[29] F. P. Koffyberg, F. A. Benko, *J. Appl. Phys.* **1982**, *53*, 1173 – 1177.
[30] Y. P. Varshni, *Physica* **1967**, *34*, 149 – 154.
[31] I. B. Krynetskiĭ, B. A. Gizhevskiĭ, S. V. Naumov, E. A. Kozlov, *Phys. Solid State* **2008**, *50*, 756 – 758.

